Journal of the European Ceramic Society 16 (1996) 195–201

0955-2219(95)00148-4
0955-2219/96/$15.00

Time-Resolved Fluorescence Spectroscopy of Cr^{3+} in Mullite

Bernard Piriou,[a] Helmut Rager[b] & Hartmut Schneider[c]

[a]PCM/URA 1907-CNRS, Ecole Centrale de Paris, F-92295 Châtenay-Malabry Cedex, France
[b]Institut für Mineralogie, Universität Marburg, D-35032 Marburg, Germany
[c]German Aerospace Research Establishment, Institute for Materials Research, D-51140 Köln, Germany

(Accepted 22 July 1995)

Abstract

Mullites doped with Cr_2O_3 concentrations ranging from 2 to 10 wt% were investigated by both time-resolved emission spectroscopy and site-selective excitation. The emission decays are non-exponential. They depend on Cr concentration and emission frequency and, hence, it is possible to distinguish different kinds of Cr^{3+} sites: at least two different types of low field site, one type of high field site and one intermediate field site. The emission decay time for Cr^{3+} in intermediate field sites was found to be the longest. In Cr_2O_3-poor mullites Cr^{3+} occurs dominantly at high field sites, i.e. at structural M(1) positions replacing Al^{3+}, whereas in Cr_2O_3-rich mullites the majority of Cr^{3+} is incorporated in interstitial sites.

1 Introduction

In recent years, mullite has attracted much interest because of its favourable high temperature properties such as low thermal expansion and conductivity, and because of its excellent creep resistance up to 1400°C.[1] Furthermore, chromium-doped mullite transparent glass-ceramics are promising compounds for tunable solid-state lasers. Mullite is able to incorporate a variety of transition metal cations into its structure. Among these ions Cr^{3+} is of special interest since it can be used as local probe for optical and electron paramagnetic resonance (EPR) investigations. Previous optical studies of chromium-doped mullite were carried out on glass-ceramics having Cr^{3+} concentrations between 0·1 and 0·05 wt% Cr_2O_3.[2–7]

The energy levels of $Cr^{3+}(d^3)$ in an octahedral field are given by a Tanabe–Sugano diagram: some levels such as $^4T_2(t_2^2e)$, $^4T_1(t_2^2e)$ and $^4T_1(t_2e^2)$ depend strongly on the crystal field strength Dq. If Dq is larger than ~1550 cm^{-1} ($Dq/B = 2{\cdot}1$) the lowest excited state is $^2E(t_2^2e)$ and Cr^{3+} is located in so-called high field sites (HFS). With $Dq < 1550$ cm^{-1}, $^4T_2$ becomes the lowest state and Cr^{3+} is located in so-called low field sites (LFS). The ground state is $^4A_2(t_2^3)$. Depending on Dq, the HFS transition $^2E \Rightarrow {}^4A_2$ and the LFS transition $^4T_2 \Rightarrow {}^4A_2$ can be observed by emission spectroscopy. The LFS transition leads to a broad band decaying in a few μs. In crystalline phases the HFS transition exhibits two sharp R-lines with lifetime in the ms region. The intensity is low because the transition is spin-forbidden. The breaking of the selection rule is due to spin–orbit coupling and phonon–electron interaction which admixes the $^4T_2$ wave function into the ^2E state and vice versa. In aluminosilicates, glasses and in more or less ordered crystalline compounds this mixing is stressed because Dq lies in the crossing region of the $^4T_2$ and ^2E states, leading to a strong distortion of oscillator strength and of the lifetime of the excited levels.[2,8–12]

Luminescence measurements of solids are helpful in the study of laser material and the search for new phosphors, because information is provided about the local structure of optically active ions in the host material, e.g. point group symmetry and crystal field strength can be inferred. In structurally disordered materials such as glasses and compounds with ion vacancies, the site-selective excitation technique is able to develop the individual response of optically different ions from an inhomogeneously broadened luminescence spectrum. Moreover, overlapping bands can often be discriminated by time-resolved spectroscopy provided the emitting levels have different decay times. In the investigation of ceramics, it was shown that the application of both techniques is suitable to follow the martensitic transformation in partially stabilized zirconia.[13]

This paper presents time-resolved fluorescence measurements of mullite with chromium concen-

trations between 2 and 10 wt% Cr_2O_3 using both these techniques, to determine structurally different Cr sites in mullite.

2 Experimental

2.1 Sample synthesis

Mullite samples were prepared by reaction sintering. Chemically pure powders of α-Al_2O_3 (62 – x wt%), SiO_2 (38 wt%) and x = 2, 5, 7·5 and 10 wt% Cr_2O_3 were used for the syntheses. After grinding the starting powders with ethyl alcohol in an agate mortar, the mixture was annealed in a PtRh crucible at 1650°C for 10 days. The glass phase present after the reaction sintering process was leached with an HF/HCl acid solution. The chemical composition and the lattice parameters of the samples are compiled in Table 1. Samples are designated as CR2, CR5, CR7·5 and CR10, according to their bulk Cr_2O_3 contents. The acid-treated mullite powders are green in colour. Samples were checked prior to spectroscopic measurements with a polarizing microscope and by X-ray diffraction. Neither impurity minerals nor glass was observed in the samples. Therefore, the acid-treated material is considered to be single-phase mullite.

2.2 Luminescence measurements

The fluorescence spectra were measured with a 80 cm double grating spectrometer (Coderg Co., PhO model) equipped with an R 928 Hamamatsu photomultiplier. The signals were processed by a Tektronix 2430 digital oscilloscope and a BFM 187 personal computer. Time-resolved measurements were performed by ultraviolet (UV) pulsed excitation using a nitrogen laser (Jobin Yvon ISA, LAO4 model). Selected excitation in the visible region was performed by a dye laser (Jobin Yvon, EIT model) pumped by a nitrogen laser. Usual dyes, coumarins, rhodamines and blue nile, were used.

Each fluorescence decay, following the excitation pulse, was analysed in real time while simultaneously scanning the wavelength of the The signals were numerically integrated in different time gates, each one defined by a given delay and width. Using up to six time gates the corresponding time-resolved emission spectra could be recorded during one scan. Each spectrum was normalized to its main band. The spectra were not corrected for the spectral sensitivity of the optical set-up. Since the cut-off of the spectrometer is near 11 000 cm^{-1}, the signals below 12 000 cm^{-1} did not have the true line shape. In order to reduce the energy transfer between chromium ions, most of the measurements were carried out at 77 K. Moreover, from this set-up, decay profiles were obtained by averaging over some hundred decay measurements.

3 Results

As reference for a Cr^{3+} high field site spectrum, the optical absorption of ruby was measured. The $^4A_2 \Rightarrow {}^4T_2$ and $^4A_2 \Rightarrow {}^4T_1$ transitions were observed as broad bands at 18 300 and 25 000 cm^{-1}, respectively. Weak narrow features in the spectrum correspond to spin-forbidden transitions from the ground state to the states ^2E, $^2T_1$ and $^2T_2$. In the absorption spectra of the samples investigated here two doublets can be distinguished. Their intensities correspond to the Cr concentration. The two doublets occur at 16 280/22 440 cm^{-1} and 18 520/24 520 cm^{-1}, respectively. By comparison with the ruby spectrum they were assigned to both low field site and high field site transitions.

Under UV pulsed excitation using a wavelength of 337 nm (29 674 cm^{-1}) all samples show a broad emission band designated as E (Fig. 1). The maximum lies at about 21 300 cm^{-1} and the line width is ~5000 cm^{-1}. The time decay of band E is < 50 ns. Below 15 000 cm^{-1} the intensity of the emission spectra depends slightly on the Cr concentration. This was not observed for sample CR2. Therefore, the concentration quenching seems to start with Cr_2O_3 contents > 2 wt%. Sample CR2 exhibits further an emission spectrum in the low energy range which differs in some details from the spectra of the samples with higher Cr content. For delay times ranging from 2 to 500 μs, two bands centred around 12 550 and 13 950 cm^{-1}, labelled as A and C respectively, were observed; band A exhibits the

Table 1. Chemical composition and lattice parameters of Cr_2O_3-doped mullites

Sample	*Chemical composition (wt%)*			*Lattice parameters (Å)*			
	Al_2O_3	SiO_2	Cr_2O_3	a	b	c	v ($Å^3$)
CR2	68·8 (3)	28·9 (4)	2·3 (2)	7·5498 (7)	7·6951 (7)	2·8867 (2)	167·71 (1)
CR5	65·7(4)	28·5 (4)	5·7 (2)	7·5561 (2)	7·7006 (2)	2·8921 (1)	168·281 (5)
CR7·5	62·8 (4)	28·4 (3)	8·6 (2)	7·5624 (4)	7·7067 (5)	2·8973 (2)	168·861 (1)
CR10	60·0 (4)	28·4 (3)	11·5 (2)	7·5674 (5)	7·7089 (7)	2·9010 (2)	169·23 (2)

The chemical composition refers to electron microprobe analyses. Values in parantheses are standard deviations. Data were taken from Rager *et al.*[7]

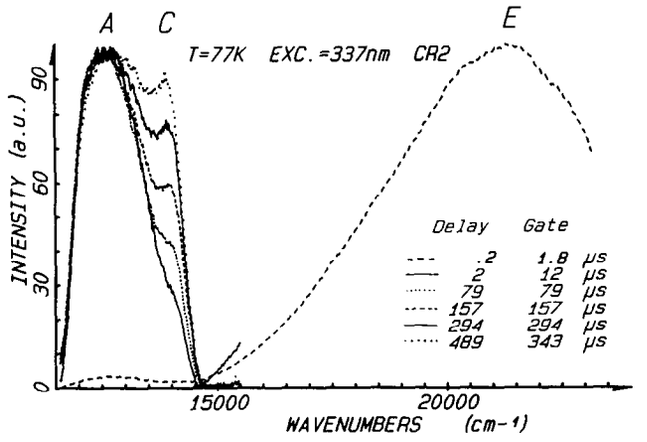

Fig. 1. Time-resolved emission spectra of sample CR2 at 77 K obtained with different delay and gate times. Excitation at 29 674 cm^{-1}.

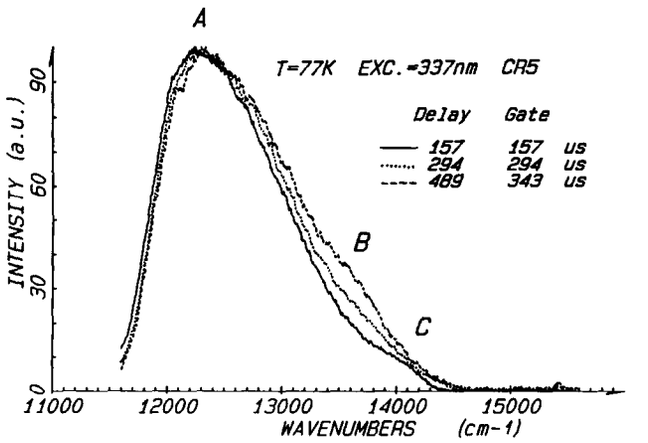

Fig. 3. Time-resolved emission spectra in sample CR5 observed with long delay times. Excitation at 29 674 cm^{-1}.

shorter decay time. Similar bands at 12 500 and 14 325/14 300 cm^{-1} were also reported from transparent mullite glass ceramics with Cr concentrations < 0·1 wt% Cr_2O_3.[2,3,5]

Band A occurs in all our samples. Except for sample CR2, it is shifted towards lower energy by increasing the delay time from 0·1 to ~20 μs (Fig. 2). The shift occurs mainly within the first 10 μs. It depends also on the Cr concentration, i.e. it increases from sample CR5 to sample CR10. In the emission spectra of samples CR5 and CR7·5, additionally, a shoulder appeared at delay and gate times of 150 μs. It corresponds probably to band C observed in sample CR2 (Fig. 1). On increasing the delay and gate times further, another shoulder designated as B appears at about 13 600 cm^{-1} (Fig. 3). In the spectrum of sample CR10, however, no indication for the shoulders B and C could be observed when delay and gate times were > 150 μs.

The decay profiles of all samples were recorded at room and liquid nitrogen temperatures; decay profiles of sample CR2 were recorded also at 22 K. The decay profiles depended on Cr concentration, temperature and observation frequency

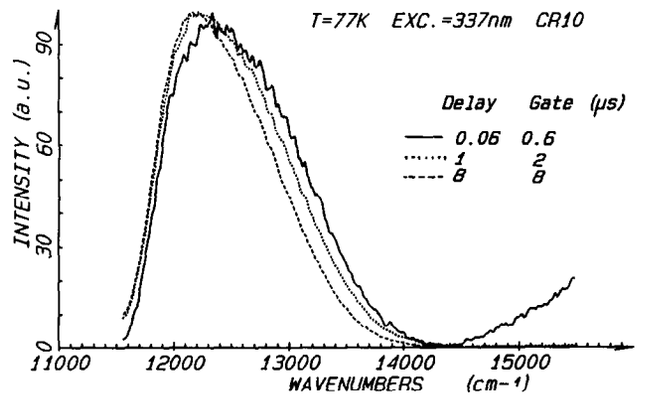

Fig. 2. Time-resolved emission spectra of band A in sample CR10 observed with short delay times. Excitation at 29 674 cm^{-1}.

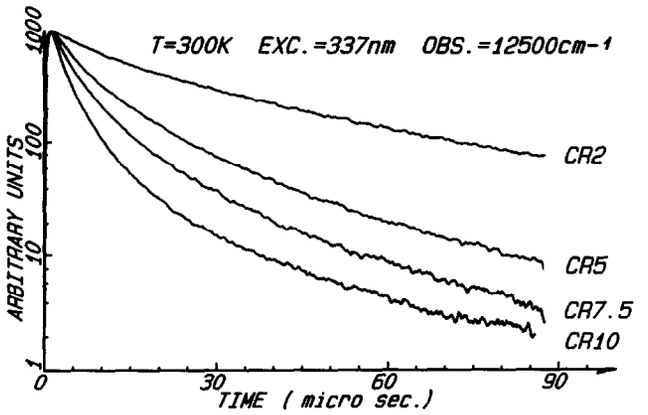

Fig. 4. Fluorescence decay profiles of band A in the different samples. Excitation at 29 674 cm^{-1}; observation at 12 500 cm^{-1}.

(Figs 4 and 5) but only slightly on the excitation frequency. All decays are non-exponential and, hence, can be characterized by a short and a long lifetime component. The short component corresponds to an average lifetime in the first e-folding while the long-lived component governs the last recorded e-folding. Both lifetime components decrease with increasing Cr content and increase with decreasing temperature. For example, in samples

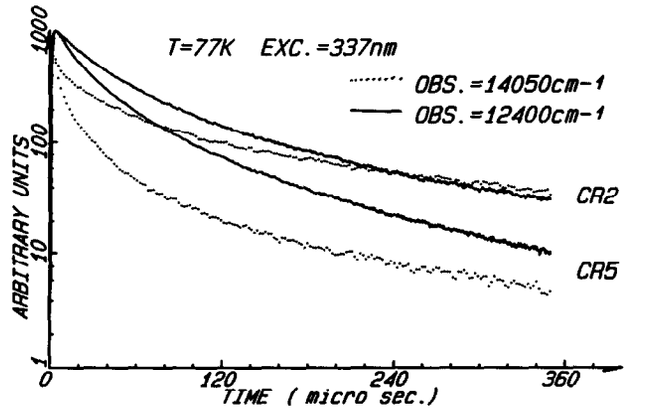

Fig. 5. Dependence of the fluorescence decay profiles on observation frequency and Cr^{3+} content at 77 K. Excitation at 29 674 cm^{-1}; observation at 14 050 cm^{-1} (dotted lines) and 12 400 cm^{-1} (full lines).

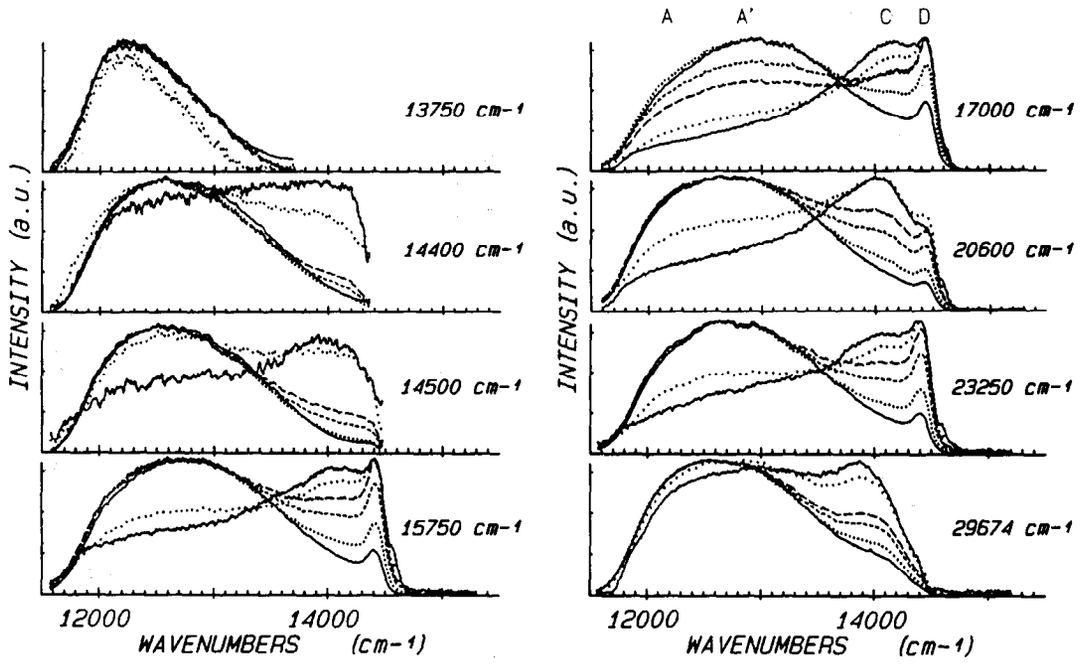

Fig. 6. Time-resolved emission spectra of sample CR2 as a function of the excitation frequency at 77 K. Gate/decay times in μs are: ——, 10/50; ....., 50/100; – – – –, 100/170; -- -- -- --, 150/150; ○○○○○○, 300/300; and ——, 500/300.

CR2 and CR10 the short lifetime components of band A are ~15 and 3 μs, respectively, at 300 K, and 30 and 5 μs at 77 K. The long lifetime components for CR2 and CR10 are 45 and 35 μs, respectively, at room temperature and 70 and 54 μs at 77 K. The non-exponential behaviour of the decay profiles does not change very much with temperature and becomes almost constant below 100 K.

Below 15000 cm^{-1} the emission spectrum of sample CR2 is strongly time-dependent. Therefore, it was investigated in detail at 77 K varying the excitation energy from 29674 to 13750 cm^{-1} (Fig. 6). To compare the spectra the time-resolved emissions during each scan were recorded with the same set of delays and gates, i.e. with 10/50, 50/100, 100/170, 150/150, 300/300 and 500/350 μs. Four bands centred at 12350 (A), 12800 (A'), 14100 (C) and 14480 (D) cm^{-1} could be resolved. The intensity ratio of these bands depends on both the time elapsed after the excitation pulse and the excitation frequency. Due to the strong deviation from an exponential decay, the lifetimes could not be determined. The bands were, therefore, classified in the sequence A', A, D and C according to their increasing decay time. The decay times range from some hundred μs to ms.

Band A could still be excited at 13700 cm^{-1}, which indicates a Stokes shift of ~1500 cm^{-1}. The lowest excitation frequency for band A' was not determined since A and A' were not time-resolved under excitation in the 13700–15000 cm^{-1} range. The width of the A–A' signal, however, is enlarged with increasing excitation energy. In contrast to the fast-decaying bands A and A', the Stokes shift of

Table 2. Summary of experminental data. Band frequencies are given in cm^{-1}

Material	$^2E \Rightarrow {}^4A_2$ *Emission*	$^4A_2 \Leftrightarrow {}^4T_2$ *Emission*	*Absorption*	$^4A_2 \Leftrightarrow {}^4T_1$ *Emission*	*Absorption*	*Assignment*	*Reference*
Glasses*		12000–12600	15200–15900		22600–23300	LFS	2, 3, 10, 14, 15
Mullites**	14280–14390	13300–13700+	16700–17200		≈25000	HFS	2, 3, 4, 5, 15
Kyanite	14180		≈17150		≈23900	HFS (A)	9
	14210	13250				HFS (B)	9
		12400	≈16240		≈23150	LFS (C)	9
Sillimanite		12000				LFS	8
Ruby	14417–14446		18300		25000	HFS	This work
CR2	14480 (D)		18520	>21300	24520	HFS	This work
CR2		14000 (C)				IFS	This work
CR5, CR7·5		13600 (B)				IFS	This work
CR2		12350 (A)	16280	<21300	22440	LFS	This work
CR2		12800 (A')	16280			LFS	This work

*Silicate and other oxide glasses.
**Cr poor mullites originated in crystallization of aluminioborosilicate glasses.
+Band maximum depends on excitation frequency, attributed to IFS.

the two long-lived bands, C and D, was estimated to be < 300 cm^{-1} because these bands could still be excited at 14400 and 14500 cm^{-1}, respectively. The intensity of the long-lived and narrow band D runs through a minimum at the excitation frequency of 21000 cm^{-1}. It could not be excited at the energy of 29674 cm^{-1}. The spectroscopic data are listed in Table 2 and compared with literature data of some reference samples.

4 Discussion

The fast-decaying, high frequency emission band E was observed in all samples. It is assigned to the $^4T_1 \Rightarrow {}^4A_2$ spin-allowed transition and corresponds to the main absorption band at 24520 cm^{-1}. The Stokes shift is ~3000 cm^{-1}. This value is of the same order as observed for $^4T_2 \Rightarrow {}^4A_2$ transitions in silicate glasses.[13] For both these transitions, which occur between the t_2^3e and t_2^3 configurations, electron–phonon coupling has to be taken into account. The Stokes shift of 3000 cm^{-1} includes (i) twice the maximum frequency of the involved phonons (relevant to the Huang–Rhys parameter) and (ii) the inhomogeneous broadening of the zero phonon line due to a distribution of Cr sites for which the crystal field continuously varies. This interpretation is supported by the band width of 5000 cm^{-1}, which indicates a convolution of the state density of the involved phonons with the inhomogeneous zero phonon band. Moreover, both high and low field chromium sites may contribute to the unusual broadening of the zero phonon band. Because of the lack of spectral and time resolution inside the E band, the above-mentioned contributions cannot be separated. A similar band width for the $^4A_2 \Rightarrow {}^4T_2$ absorption was reported for transparent mullite glass-ceramics.[15]

In sample CR10 only band A is observed. According to its low energy, this fast-decaying band is ascribed to $^4T_2 \Rightarrow {}^4A_2$ transitions of Cr^{3+} in low field sites. The shoulder B, clearly observable only when the delay times were > 500 μs and occurring only in the spectra of samples CR5 and CR7·5, is difficult to assign. The long decay time could be indicative of high field sites; however, the band width and the energy of the shoulder rules out this possibility. Band C appears at intermediate delay times of ~150 μs and does not occur at other delay times. Regarding the intensities of the bands A, B and C, the dominant band A suggests that predominantly low field sites of Cr^{3+} exist in the samples CR5, CR7·5 and CR10.

In spite of the energy transfer due to different non-radiative relaxation processes, the emission spectra of CR2 show a significant degree of site selection which is emphasized by the kinetic behaviour as shown in the spectra of Fig. 6. The time-resolved spectra reveal the presence of two bands, A and A', in the low energy range. The decay of A and A' is fast and, hence, they are assigned to $^4T_2 \Rightarrow {}^4A_2$ transitions of two families of chromium low field sites. In previous investigations,[3,5,15] only one band at about 12500 cm^{-1} was observed in this energy range. As for the E band this interconfigurational transition ($t_2^2e \Rightarrow t_2^3$) is phonon-assisted. The Stokes shift of 1500 cm^{-1} for band A was estimated from the limit of the site-selective excitation. It is significantly smaller than the Stokes shift of band E. This may be explained by assuming that only a small fraction of Cr^{3+} centres within a given distribution of low field sites was excited. In such a case the band width may be reduced to its homogeneous width. Furthermore, the excitation can still occur with low energy phonons, i.e. close to the zero phonon line.

The sharp long-lived band D at 14480 cm^{-1} is close to the ruby R-lines at 14417 and 14446 cm^{-1}. It is, therefore, attributed to transitions between the states ^2E and $^4A_2$ which belong to Cr^{3+} ions at high field sites. The transition $^2E \Rightarrow {}^4A_2$ occurs within the t_2^3 configuration and is not vibronically broadened. Its inhomogeneous width of about 120 cm^{-1} indicates a certain variation of high field sites. The low fluorescence efficiency and the strong diffuse reflectance did not allow to observe resonantly this transition, but close to the excitation at 14500 cm^{-1} the emission band appears at 14400 cm^{-1}. Thus, the Stokes shift of $\simeq$100 cm^{-1} or even less indicates a weak phonon coupling.

The A/A' and D bands are usually encountered in silicate and aluminosilicate ceramics as well as in the corresponding glasses.[2,4,5,14,15] They were identified without difficulty. In contrast, the origin of the C band around 14000 cm^{-1} is not clear. So far this band has not yet been mentioned in the literature, except for a band at 13700 cm^{-1} in a transparent glass-ceramic.[14] The decay of C band is longer than the decay of high field site transitions between ^2E and $^4A_2$. The maximum frequency as well as the band width of about 800 cm^{-1} classify it just between LFS and HFS emissions. It is still present under a 14400 cm^{-1} excitation, which indicates a Stokes shift of ~400 cm^{-1}. We ascribe it, therefore, to intermediate field sites (IFS) of Cr^{3+} for which the crystal field parameters lies in the crossing region of the $^4T_2$ and ^2E states. Nevertheless, the long decay and the small Stokes shift are not well understood. A distribution of Cr^{3+} at intermediate field sites was already mentioned by some authors[5,15] and, hence, an emission from both $^4T_2$ and ^2E states may be expected. The intermediate field sites of Cr^{3+} are not restricted to

centres which obey the condition $\Delta E = {}^4T_2 - {}^2E = 0$.$Cr^{3+}$ energy states which differ at 77 K from the above condition by less than ± 100 cm^{-1} may be activated thermally to emit from the two levels. Further, the states $^4T_2$ and ^2E should be in thermal equilibrium and, thus, emission from both levels should occur with the same decay. However, this consideration may not apply to bands D and C because they show a different time behaviour. Moreover, as pointed out by Andrews *et al.*,[15] a two-level thermally equilibrated system could not be applied to the data obtained for Cr^{3+} in transparent glass-ceramics in the temperature range 77 to 298 K. A more sophisticated model,[11] with adequate parameters, and which includes spin–orbit and vibronic coupling effects in the crossing region, is needed to explain the nature of the C band. The admixture of wave functions with predominant ^2E character, for example, could explain the long lifetime. Furthermore, a certain separation between the ^2E and $^4T_2$ branches in the coupling region may explain the lowering of the emitting level with respect to the pure ^2E level and the fact that no emission from the upper level occurs.

The intensity calibration of the time-resolved emission spectra was difficult because the intensities of the dye lasers are wavelength-dependent. Seven different dyes were required for the excitation beam to cover the range from 13 500 to 23 500 cm^{-1}. Further, reproducibility of the optical set-up was hard to achieve. Therefore, the selectivity of the spectra with respect to the individual chromium sites in mullite was estimated by the intensity ratios $(I_{14480}/I_{12900})_2$ and $(I_{14000}/I_{12900})_4$ of the bands D, C and A'. The subscripts 2 and 4 denote the second and fourth gates (see Fig. 6) through which bands D and C could best be resolved. The ratios (Fig. 7) reflect the spectral selectivity of the long-lived bands with respect to the fast-decaying bands, i.e. HFS/LFS ratios. The curves in Fig. 7 correspond roughly to the absorption spectrum of both high and low field chromium sites. Although the experimental accuracy of these plots is not high, two small dips at 14 600 and 14 800 cm^{-1} should be noted. A similar fine structure also appeared in the $^4A_2 \Rightarrow {}^4T_2$ absorption band in Cr-doped glasses.[10,14] The most probable interpretation is a Fano anti-resonance between the $^4T_2$ vibrational quasi-continuum and the $^2T_1$ and ^2E discrete levels.

In the mullite sample with the lowest Cr_2O_3 content, bands D and C indicate high and intermediate field sites and bands A and A' two kinds of low field site. This corresponds to the observations in mullite glass-ceramics with low Cr contents which exhibit high and low field sites, though the major part of Cr^{3+} may occur in high

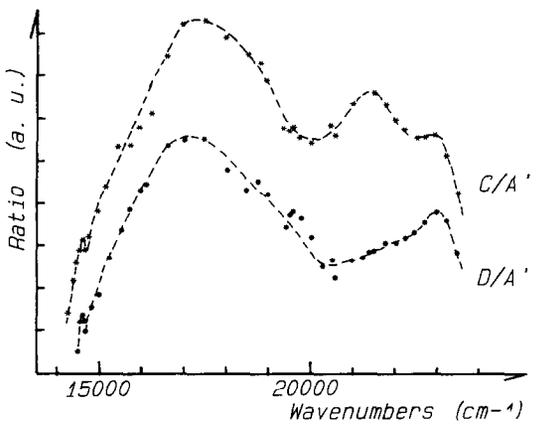

Fig. 7. Spectrum of the excitation ratios C/A' and D/A' bands in sample CR2 at 77 K.

field site domains.[4] In mullites with intermediate and high Cr_2O_3 contents only the band A can be clearly observed. The results are interpreted in the following way: at low Cr_2O_3 contents the predominantly high field Cr sites are explained by Cr^{3+} at octahedral M(1) positions (position (2*a*) in the space group *Pbam* of mullite). With increasing Cr concentration in the mullite structure, low field Cr sites predominate which are described as distorted interstitial Cr sites. The fluorescence spectroscopic results presented here, i.e. the occurrence of at least two different structural Cr sites in mullite, agree well with spectroscopic investigations by electron paramagnetic resonance (EPR) and by optical absorption.[1,7]

Finally, we would like to comment on the non-exponential behaviour of the band decays observed in all samples. This observation is not surprising because it was likewise reported for transparent mullite glass-ceramics.[5,15] It is explained by an excitation transfer between the Cr^{3+} ions which increases with increasing Cr content and temperature. An energy transfer mechanism from HFS to LFS was proposed in the literature.[3] However, other transfer mechanisms among Cr sites of the same kind cannot be excluded. Thus, for band A of sample CR10 (Fig. 2), which was identified as $^4T_2 \Rightarrow {}^4A_2$ transitions of low field chromium sites, a transfer from high to low energy sites within a distribution of low field sites could explain the observed shift towards lower energy as the delay time increases. Generally, excitation transfers are assumed to be responsible for the poor selectivity when applying site-selective excitations, as can be seen in Fig. 6.

5 Conclusion

In this work time-resolved fluorescence spectroscopy was applied in a wide time range to investi-

gate Cr sites in heavy doped mullite. $^4T_2 \Rightarrow {}^4A_2$, $^4T_2 \Rightarrow {}^4A_2$ and $^2E \Rightarrow {}^4A_2$ emissions were separated. As in low Cr content mullite glass-ceramics, high and low field chromium sites have been detected. The further findings are summarized as follows.

1. At least two types of low field chromium site occur in the mullite structure.
2. In addition to the 14480 cm^{-1} band which is attributed to high field chromium sites, another band at 14000 cm^{-1} with the longest observed decay time appears. It is assigned to intermediate field chromium sites. The ^2E character of the emitting level of this band is retained despite its unusual low energy.
3. In mullites containing high Cr_2O_3 contents, Cr^{3+} ions are mostly located in low field sites with a certain variation of their crystal fields. All sites have the $^4T_2$ state as the lowest level.
4. High field Cr sites are predominant in Cr_2O_3-poor mullites. They are correlated with incorporation of Cr^{3+} at octahedral M(1) positions replacing Al^{3+}. Upon increasing the Cr_2O_3 content Cr^{3+} favourably enters the highly distorted low field sites, which are attributed to interstitial lattice positions in the mullite structure.
5. Strong deviation from an exponential decay is observed for all emission bands at room and low temperatures (22 K). This may be explained by an energy transfer between different Cr sites which occurs even at low temperatures.

References

1. Schneider, H., Okada, K. & Pask, J. A., *Mullite and Mullite ceramics*, John Wiley and Sons, Chichester, 1994.
2. Wojtowicz, A. J. & Lempicki, A., Luminescence of Cr^{3+} in mullite transparent glass ceramics (II). *J. Lumin.*, **39** (1988) 189–203.
3. Knutson, R., Liu, H., Yen, W. E. & Morgan, T. V., Spectroscopy of disordered low-field sites in Cr^{3+}: mullite glass ceramic. *Phys. Rev. B*, **40** (1989) 4264–70.
4. Liu, H., Knutson, R. & Yen, W.M., Saturation-resolved-fluorescence spectroscopy of Cr^{3+} mullite glass ceramic. *Phys. Rev. B*, **41** (1990) 8–14.
5. Liu, H., Knutson, R., Jia, W., Strauss, E. & Yen, W. M., Spectroscopic determination of the distribution of Cr^{3+} sites in mullite ceramics. *Phys. Rev. B*, **41** (1990) 12888–94.
6. Schneider, H., Transition metal distribution in mullite. *Ceram. Trans.*, **6** (1990) 135–58.
7. Rager, H., Schneider, H. & Graetsch, H., Chromium incorporation in mullite. *Am. Mineral.*, **75** (1990) 392–7.
8. Wojtowicz, A. J. & Lempicki, A., Luminescence of Cr^{3+} in sillimanite. *Phys. Rev. B*, **39** (1989) 8695–701.
9. Wojtowicz, A. J., Luminescence of Cr^{3+} in kyanite. *J. Lumin.*, **50** (1991) 221–30.
10. Brawer, S. A. & White, W. B., Optical properties of trivalent chromium in silicate glasses: a study of energy levels in the crossing region. *J. Chem. Phys.*, **67** (1977) 2043–55.
11. Donelly, C. J., Healy, S. M., Glynn, T. J., Imbush, G. F. & Morgan, G. P., Spectroscopic effects of small $^4T_2$–^2E energy separations in $3d^3$-ion systems. *J. Lumin.*, **42** (1988) 119–25.
12. Wojtowicz, A. J., Grinberg, M. & Lempicki, A., The coupling of $^4T_2$ and ^2E states of Cr^{3+} ion in solid state materials. *J. Lumin.*, **50** (1991) 231–42.
13. Piriou, B., Dexpert-Ghys, J., Bastide, B. & Odier, P., Martensitic transformation of TZP investigated by site selective spectroscopic method. *Proceedings of Zirconia 88*, 17 November 1988, Bologna.
14. Andrews, L. J., Lempicki, A. & McCollum, B. C., Spectroscopy and photokinetics of chromium (III) in glass. *J. Chem. Phys.*, **74** (1981) 5526–38.
15. Andrews, L. J., & Lempicki, A., Luminescence of Cr^{3+} in mullite transparent glass ceramics. *J. Lumin.*, **36** (1986) 65–74.